Proceedings World Geothermal Congress 2020+1
Reykjavik, Iceland, April - October 2021

Developing a Conceptual Model of One of Three Geothermal Prospects at Hawthorne, Nevada, USA

Bridget Ayling[1], Nicholas Hinz[1], Kelly Blake[2], Andrew Sabin[2], Thomas Lowry[3] and Andrew Tiedeman[2]

[1] Great Basin Center for Geothermal Energy, NBMG, University of Nevada, Reno, 1664 N. Virginia St, Reno, NV 89557, USA

[2] Navy Geothermal Program Office, 429 E. Bowen Road, China Lake, CA 93555, USA

[3] Sandia National Laboratories, P.O. Box 5800 MS 1137, Albuquerque, NM 87185, USA

bayling@unr.edu

Keywords: Direct-use; Hawthorne; Walker Lane; conceptual model; low-temperature; Nevada

ABSTRACT

The Hawthorne, Nevada area in the western part of the Basin and Range province in the western USA has been the focus of geothermal investigations for over 40 years, with initial discovery of blind resources via anomalously warm water wells. Subsequent studies and drilling of temperature gradient holes and geothermal wells identified three separate blind geothermal prospects in the Hawthorne part of the Walker Lake basin. In 2017, the US Department of Energy funded a project to investigate the feasibility of installing deep, direct-use geothermal technology at the Hawthorne Army Depot and adjacent community of Hawthorne. For this project, we conducted a detailed review of all existing geoscience data acquired at the site to date to develop a quantitative estimate of geothermal resource potential for one of the Hawthorne geothermal prospects (prospect A – along the southwest side of the basin). This included review of substantial well data from water wells and geothermal exploration wells (downhole temperature logs, lithology, water chemistry, borehole televiewer, and alteration mineralogy), detailed geological and structural mapping information, geophysical data (gravity, magnetic, and seismic reflection), 2 m temperature data, and an existing 3D geological model of the basin.

We find that the thermal anomalies associated with prospect A reflect the influence of two, related geothermal fluids in close proximity that are chemically distinct, with different temperatures and spatial extent (lateral and vertical). One fluid represents a deeper resource, hosted in altered, fractured Mesozoic granitic basement along a segment of the Wassuk Range-front fault system, and characterized by mature, alkali-chloride fluids, with ~4000 ppm total dissolved solids (TDS) and a maximum measured temperature of ~115 °C at ~1,500 m depth. A second fluid is hosted in Neogene basinal sediments at <400 m depth, with maximum measured temperatures of ~100 °C, TDS of ~1000 ppm, and a sodium-sulfate fluid chemistry. The outflow of this shallow resource can be tracked down gradient into the basin using well temperature data, which map a vertically constrained plume that cools with distance from the inferred upflow location. The data suggest that the deeper resource is conductively transferring heat to the shallow resource, and structural and/or stratigraphic compartmentalization is preventing direct interaction and fluid mixing. Here we integrate the data to develop a new conceptual model of prospect A, including the P10, P50, and P90 scenarios, and compare this with previous conceptual models developed for Hawthorne.

1. INTRODUCTION

The Hawthorne geothermal area is in the Walker Lake basin in the western part of the Great Basin, USA, and has been the focus of geothermal exploration efforts for over 40 years (Figure 1). It contains several blind geothermal systems with no surface thermal manifestations and were first discovered in the 1940's and 1950s during drilling of water wells. Targeted geothermal exploration efforts did not begin until the mid-1970's and have continued sporadically through to the present day. Key exploration activities conducted to date include the drilling and logging of multiple thermal gradient wells and deeper slim-holes, 2 m temperature surveys, gravity, 3D reflection seismic and LiDAR data acquisition, detailed geological and structural studies, and fluid geochemistry sampling from wells in the basin. There are three known geothermal anomalies (prospects) in the basin identified through this previous work – prospects A, B and C (Hinz et al., 2010) (Figure 2). Downhole temperature logs indicate that these three systems are low-temperature (< 120 °C), and at least two of the three have shallow outflow plumes as observed in temperature logs. With the exception of prospect A, the locations of geothermal up-flow for these three anomalies are poorly constrained.

In 2017, the US Department of Energy issued a funding opportunity with a focus on direct-use applications of geothermal resources in the USA. The goal of the funding initiative was to conduct techno-economic feasibility assessments of potential direct-use systems at prospective locations, incorporating the geothermal resource constraints as well as the below-ground and above-ground engineering components, and economic considerations. The Hawthorne site was proposed for such a feasibility assessment, given its proven resource potential and long history of exploration, and the opportunity to utilize the geothermal resource for direct-use applications at the Hawthorne Army Depot (HAD) (a government-owned and contractor-operated military facility), and in the Hawthorne community (total population <3300 people). The project was awarded and began in late 2017, with an expected completion by the end of 2019 (see Blake et al., 2017; Arguello et al., 2018; Sabin et al., 2018). For the project, prospect A was prioritized as the potential resource, given its more-comprehensive subsurface dataset (including well-test data), and proximity to the HAD and town of Hawthorne (Figure 2).

We evaluated the potential resource capacity of prospect A in terms of temperature, fluid production rates and reservoir size/volume, through review and integration of the existing geoscientific data for the area, and development of new resource conceptual models at different levels of certainty (but always honoring the data). In this paper, we present a new conceptual model of the geothermal resource at prospect A, as well as the key uncertainties and data gaps associated with this conceptual model.

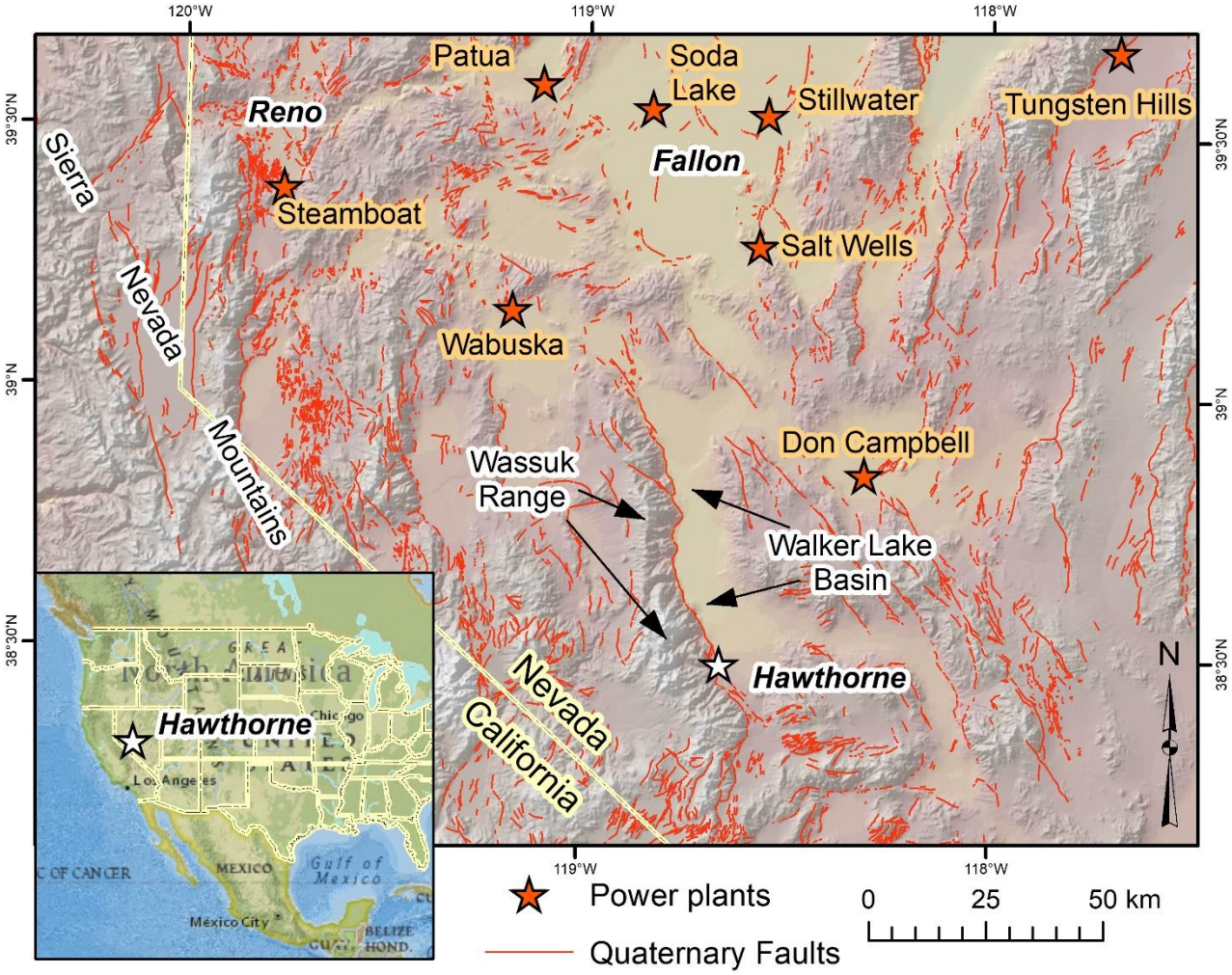

Figure 1: Regional map illustrating the location of Hawthorne relative to other geothermal sites in Western Nevada. Inset: location of Hawthorne in the western USA.

2. GEOLOGIC SETTING

The Hawthorne area is located along the western side of the central Walker Lane (e.g., Faulds and Henry, 2008) in the Basin and Range province, and straddles the southern part of the Walker Lake basin, extending east into the northwestern Garfield Hills, and west into the south-central part of the Wassuk Range (Figure 2). The ~80 km-long Walker Lake basin marks a major physiographic break along the western boundary of the Walker Lane, coincident with a transition between a region dominated by NW-striking dextral strike-slip faults to the east and a region dominated by N- to NW-striking normal and dextral-oblique faults extending westward to the Sierra Nevada (Hardyman and Oldow, 1991; Oldow, 1992; Proffett, 1977; Proffett and Dilles, 1984; Stewart, 1988; Wesnousky, 2005).

The stratigraphic framework consists of Neogene volcanic and sedimentary deposits that rest on Mesozoic granite and metamorphic basement. The Neogene strata reach up to 1.7 km-thick in the Walker Lake basin and consist of four primary sequences from oldest to youngest: 1) middle Miocene andesite lavas; 2) late to middle Miocene fluvial and lacustrine sediments, including local evaporites; 3) late Miocene basaltic andesite lavas and rhyolite domes, flows, and intrusions; and 4) Pliocene to recent basin fill sediments (Stockli et al., 2002; Surpless et al., 2002; Hinz et al., 2010). Tilts of these Neogene strata filling the basin are not well constrained. Several west-tilted fault blocks identified in the 3D seismic data dip gently 15° west with a decrease in dip up section. Dips range from 5 to 20° W in un-folded, late Miocene basaltic andesite that project into the basin along the west edge of the Garfield Hills (Figure 2).

The Walker Lake basin is a complex half-graben, bound on the west by the Wassuk Range-front fault system and defined to the east by a broad, gently west-dipping ramp, cut locally by west-dipping antithetic faults. Within the map area, the Wassuk Range-front fault bifurcates into two major strands from the Lucky Boy Mine area to the mouth of Cat Creek (faults A and B, Figure 3). The range-front fault system dips ~30° to 55° NE (Hinz et al., 2010). The overlap area between faults A and B is cut by numerous N- to NE-striking, east- and west-dipping normal faults with ~45-65° dips. At the south end of the basin, the ~20 km-long NW-striking dextral Willow Springs fault (informally named in this paper) splays from the Wassuk Range front near the Lucky Boy Mine area and connects with other strike-slip and normal faults at the west edge of the Garfield Hills. The Walker Lake basin half-graben is cut by multiple N- to NW-striking E- and W-dipping normal faults, including the newly identified Hawthorne fault zone that extends NNW from the step-over region of the range-front (Bell and Hinz, 2010). Much of both the Wassuk Range front fault and Hawthorne fault zones are marked by Holocene and/or Pleistocene scarps. The largest Holocene scarps are up to 10 m high at the mouth of Cat Creek.

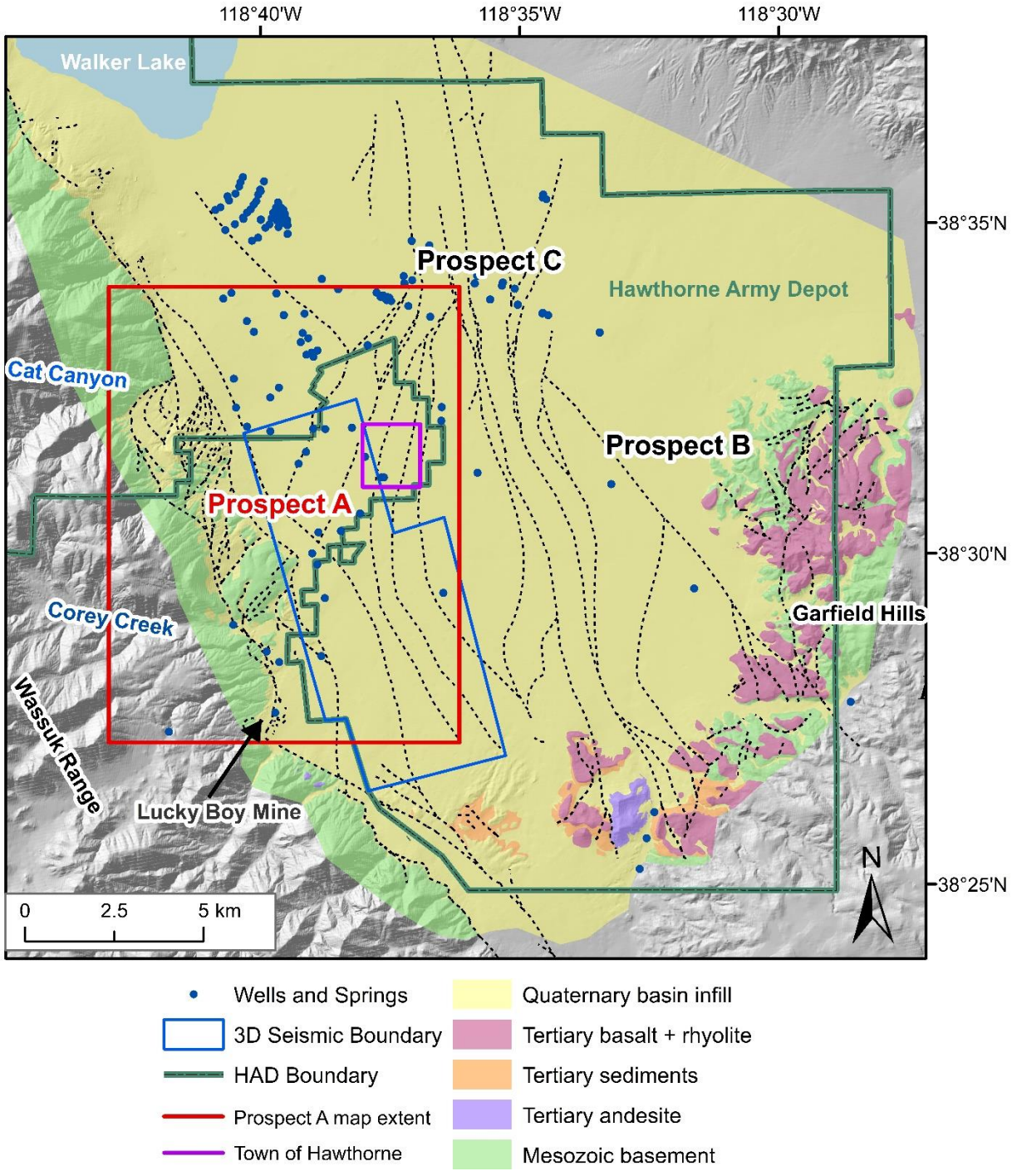

Figure 2: Semi-transparent geologic map draped over shaded relief image, and key locations mentioned in the text including the approximate area of geothermal anomalies informally called prospects A, B and C. Red box corresponds to the map extent of Figures 3, 5, and 11. Faults are represented as dotted black lines.

Exposed fault surfaces were analyzed in the area to elucidate the kinematics of fault systems, determine the orientations of principal strain and stress axes, and perform slip and dilation tendency analyses (Moeck et al., 2010). Measurements from 45 fault surfaces in the step-over part of the Wassuk Range front fault indicate a NW-SE (azimuth 127°) extension direction. Ratios of principle stresses signify a transtensional stress regime comprising both extension and dextral shear. From these data, it is expected that the Wassuk-Range-front fault has been accommodating dextral-oblique motion.

3. PREVIOUS GEOTHERMAL EXPLORATION

Anomalously warm ground water was first discovered in the Hawthorne area in the 1940's and 1950's on property that belonged to the U.S. Navy, with temperatures ranging from ~16 °C to ~52 °C (Koenig, 1981). Several studies in the late 1970's and early 1980's attempted to learn more about the potential geothermal resource and its potential for direct-use applications, including work by Bohm and Jacobson (1977a), Geothermal Development Associates (1981), Robinson and Pugsley (1981) and Koenig (1981). Bohm and Jacobson (1977a) proposed that hot water emerged along faults that transect the basement and alluvium along the Wassuk Range front, and is mixed with cooler water, flowing eastward and northward. The study by Koenig (1981) was comprehensive and included the acquisition of new data such as water geochemistry, shallow 2-meter temperature surveys, temperature logging of available wells,

soil mercury surveys, a gravity survey, low sun-angle photography to assist in identifying recent fault scarps in the basin, and drilling of two new thermal gradient wells (HHT-1 and HHT-2). Around this time (1980), a ~305 m (1000 ft) deep geothermal well was also drilled by a private landowner (El Capitan Club Estates), who hoped to use the geothermal fluids for space heating. The well was named 'El Capitan' and had a maximum measured temperature of 98 °C (210 °F). It was also subjected to pump tests to prove the aquifer transmissivity, as well as geochemical sampling.

Koenig (1981) synthesized and interpreted these data from the El Capitan well alongside those collected in their study, and other pre-existing data from the earlier studies. Key findings from this work included the observation that in surface water samples from rivers draining the east side of the Wassuk Range, and in samples from shallow water wells (< 100 m deep), sulfate concentrations increased basin ward. Additionally, a shallow temperature anomaly was mapped from the 2 m temperature data and test well data, which trended from south to north around the city of Hawthorne area. Deep geothermal fluids were speculated to rise up along permeable faults (in an area of fault intersections near the El Capitan well), and flow out in a northerly-plume hosted in the basin-infilling sediments. A second anomaly was identified just east of the Garfield Hills, but the source or conceptual model of this anomaly was not well constrained.

Continued work by the Navy's Geothermal Program Office (GPO) in the late 1990's and early 2000's to understand the geothermal resource potential of the Hawthorne area included the acquisition of new gravity and magnetic data (Katzenstein et al., 2002). These data were used in conjunction with the existing geochemistry, geological, and geophysical data to develop a conceptual model (cross section) of the geothermal resource on the eastern edge of the Wassuk Range. Key conclusions were similar to earlier interpretations proposed by Bohm and Jacobson (1977), Robinson and Pugsley (1981) and Koenig (1981). Katzenstein et al. (2002) proposed that meteoric water falling on the Wassuk Range percolates down to depths of at least 2100 m (7000 ft), is heated, and rises to the surface via faults bounding the eastern edge of the Wassuk Range. Additionally, Katzenstein et al. (2002) recommended the acquisition of a 3D reflection seismic survey to improve the mapping of subsurface structure, and to help site a deep drilling target. In 2005, the GPO conducted a 3D seismic reflection survey in an attempt to image subsurface fault patterns in a 10 square mile area extending from well HHT-1 to east of the Lucky Boy Mine (see Figure 2). Ongoing efforts by the Navy GPO culminated in the drilling of multiple wells between 2008 and 2012, including 13 thermal gradient wells (< 200 m deep), three deeper slim holes, one direct-use test hole, and later modifications to two thermal gradient holes (Lazaro et al., 2010; Meade et al., 2011; Blake et al., 2017). The deeper wells were logged, flow tested, and cuttings samples were analyzed using XRD and petrographic analysis. Additionally, the Navy GPO subcontracted the Great Basin Center for Geothermal Energy to conduct a comprehensive study of the area in 2008-2009. This included detailed geological mapping and structural analysis, developing a 3D geological model of the Walker Lake basin, interpreting the 3D seismic survey, evaluating fluid chemistry, conducting additional 2 m temperature surveys, inversion of gravity data, and evaluation of LiDAR and low sun-angle photography to identify Holocene fault scarps (Bell and Hinz, 2010; Hinz et al., 2010; Kell et al., 2010; Kratt et al., 2010; Moeck et al., 2010; Penfield et al., 2010, Shoffner et al., 2010). Key findings from this work included identifying an additional thermal anomaly in the basin (bringing the total to three), providing improved delineation of the thermal anomalies via the 2 m data and new temperature logs from the Navy exploration wells, and developing the first 3D structural and geological model of the basin (Figure 2).

4. DATA REVIEW FOR PROSPECT A

4.1 Local geology

Prospect A is centered along a 3 km-wide by 12 km-long, step-over along the NNW-striking, WNE-dipping Wassuk Range-front fault system (Figures 2, 3). The step-over consists of two major synthetic range-front fault splays (Faults A and B, Figures 2, 3) bounding an area with numerous NNE- to NE-striking faults. Range-front fault strands A and B both have local 0.5 to 1 km steps along-strike, including a near-ninety degree bend associated with a step near Ken Maples #1 well. This step near Ken Maples well is also where the NNE- to NE-striking Hawthorne fault zone projects into the Wassuk Range-front fault zone. The specific linkage or cross-cutting patterns between individual fault strands is not well understood as many fault strands are buried by Late Pleistocene or Holocene alluvium.

Both the range-front fault zone and the Hawthorne fault zone have Late Pleistocene and Holocene fault scarps, indicating relatively active Quaternary fault activity (Bell and Hinz, 2010). Borehole image log analysis and kinematic analysis of fault surface data indicate that the least principal stress extension direction is N47°W and N53°W, respectively (Hinz et al. 2010, Moeck et al., 2010; Blake, 2011). This stress field orientation could facilitate oblique motion along the Wassuk Range-front fault system and provides a basis possible enhanced permeability at discrete right steps in this fault zone.

The stratigraphic framework defined in the prospect A area includes only Miocene(?) to present basin-fill sediments and Mesozoic granite. Exposures of these sediments along the fault zones show they are composed of lacustrine sand and silt, pebble conglomerate of fluvial and lacustrine origin, and lesser evaporites and tuffs. The two slim wells, HWAAD-2A and HWAAD3, both intersect basin-fill sediments and cross-strands of the range-front fault and terminate in Mesozoic granite. From these well records and the 3D seismic data, the late Miocene basaltic andesite pinches out in this area and the middle Miocene andesite is not found this high up in the hanging-wall of the range-front fault system.

4.2 Temperature data

2-meter temperature data, downhole temperature logs and bottom hole temperature measurements were collated from existing data sources. These included data from water wells, temperature gradient holes, and three deeper geothermal exploration wells (HWAAD-2A, HWAAD-3, and 76-19) (Figure 3, Figure 4). The two deepest wells exhibit temperature profiles that are markedly different from one another: well HWAAD-2A encounters the highest temperatures measured in the Hawthorne area to date, with a 600 m-thick, 115 °C isothermal section at the bottom of the well that is interpreted to reflect fluid upflow. This well is cased and completed in the Mesozoic granite (Figure 4). In contrast, HWAAD-3 exhibits a conductive temperature profile, although it is still elevated compared to the typical regional background for the Basin and Range (~60 °C/km vs ~40 °C/km).

Several of the shallower logs have temperature overturns in their upper levels (<200 m depth), suggesting that these wells intersect a thermal outflow plume. There is also a decrease in the temperature of this overturn from south to north, from the vicinity of the El Capitan well, to TGH-1. Comparison with the 2 m temperature map illustrates anomalous temperatures that are approximately coincident with the location of this inferred shallow outflow plume (Figure 5).

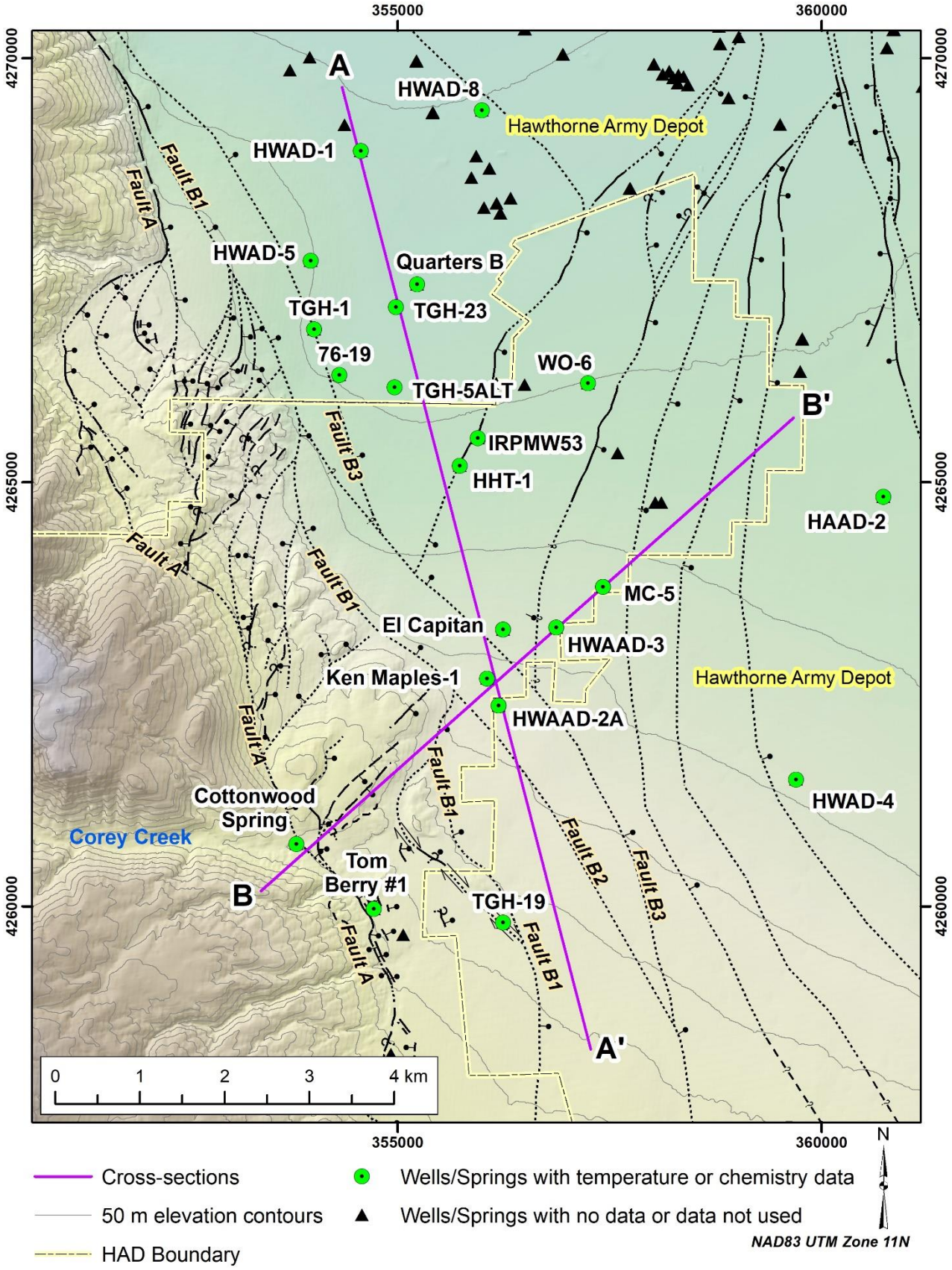

Figure 3: Location of geothermal and water wells in Hawthorne geothermal prospect A, faults, elevation contours, and cross sections that are presented in Section 5.

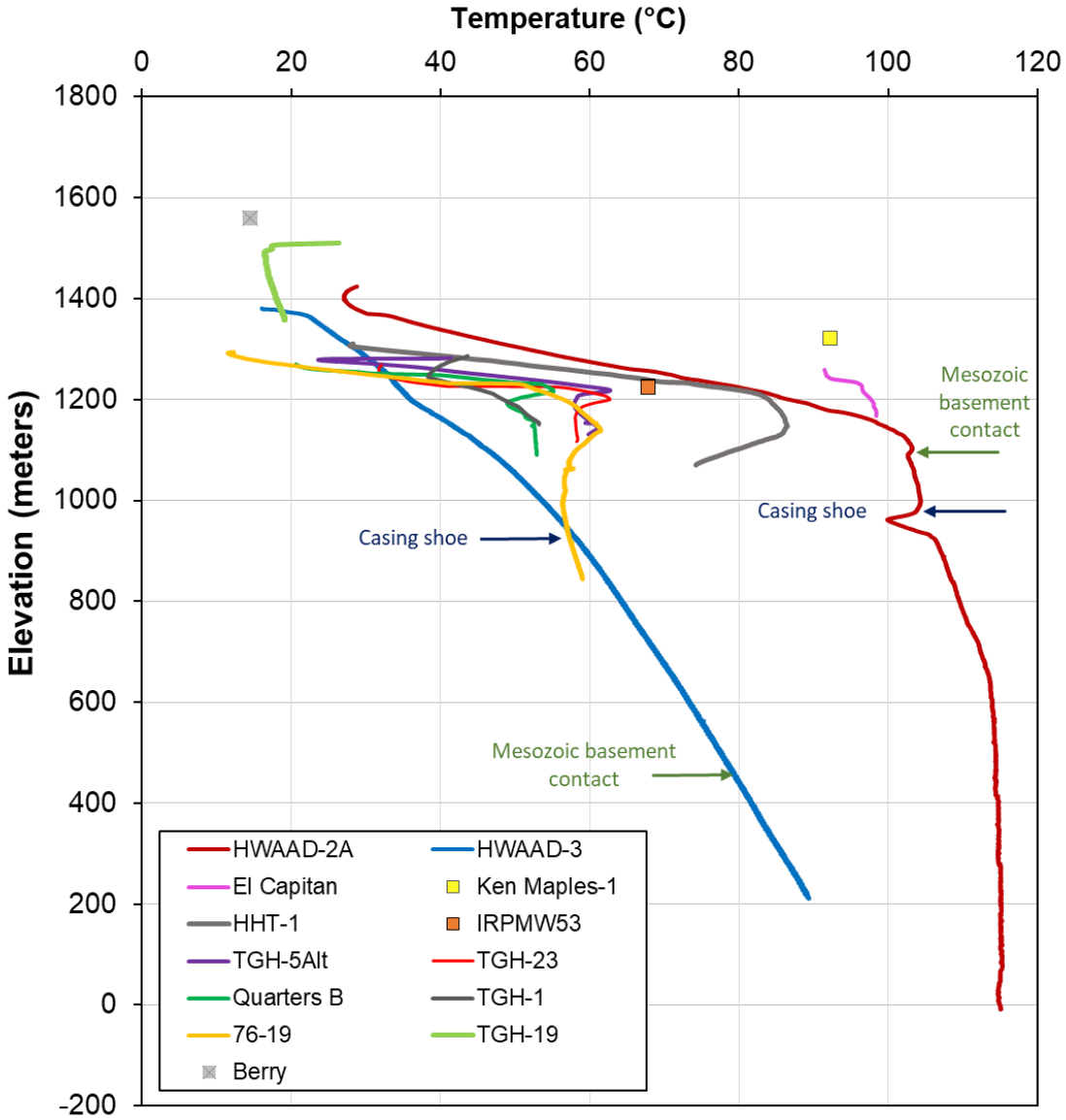

Figure 4: Downhole temperature data from wells in and adjacent to Hawthorne geothermal prospect A. The wellhead elevations decrease in a northerly direction (basin-ward) hence the offset in log elevations. The wells HWAAD-2A and HWAAD-3 are the only ones to penetrate the Mesozoic basement.

4.3 Fluid geochemistry

Water chemistry data were reviewed and compiled for prospect A: any data with charge imbalances greater than ±10 % were not used for subsequent interpretation. Initial observations identified three discrete fluid types with distinct chemical signatures (Figures 6, 7). As indicated by previous studies (e.g.: Koenig, 1981; Katzenstein et al., 2002), samples obtained from the shallow water wells in the basin and deeper geothermal wells El Capitan and Ken Maples exhibit a sodium-sulfate fluid chemistry, and generally have total dissolved solids (TDS) values between 700-1000 ppm. Samples collected from the river drainages on the eastern side of the Wassuk Range (e.g.: Corey Creek and Cottonwood Creek) have low TDS (< 235 ppm) and are bicarbonate fluids. Two samples collected from the deep well HWAAD-2A (production interval in the Mesozoic granite) are unique, with an alkali-chloride composition and much higher TDS (~4,200 ppm) (Figure 6).

The two fluid types observed in the basin (alkali-chloride and sodium-sulfate) do not exhibit any mixing trends and appear to be chemically distinct (Figures 6,7). This contrasts with the observed mixing trend between the surface water fluids and the sulfate fluids that do fall on a mixing line and is inferred to reflect the flow of relatively fresh meteoric waters from the Wassuk Range through the basin infill, where it collects more dissolved solids such as sulfate. The sulfate fluids were all sampled from wells that are less than 200 m deep and are completed in the Miocene and Pliocene basin infilling sediments, whereas the chloride fluid from well HWAAD-2A was sampled from fractured zones in the Mesozoic granite near the bottom of the well (> 1300 m depth) during flow testing of the well (GeothermEx, 2009). Thus it appears the reservoir hosting the alkali-chloride fluid is compartmentalized, and these chloride fluids are not intermixing with the sodium-sulfate fluid encountered in the shallow wells.

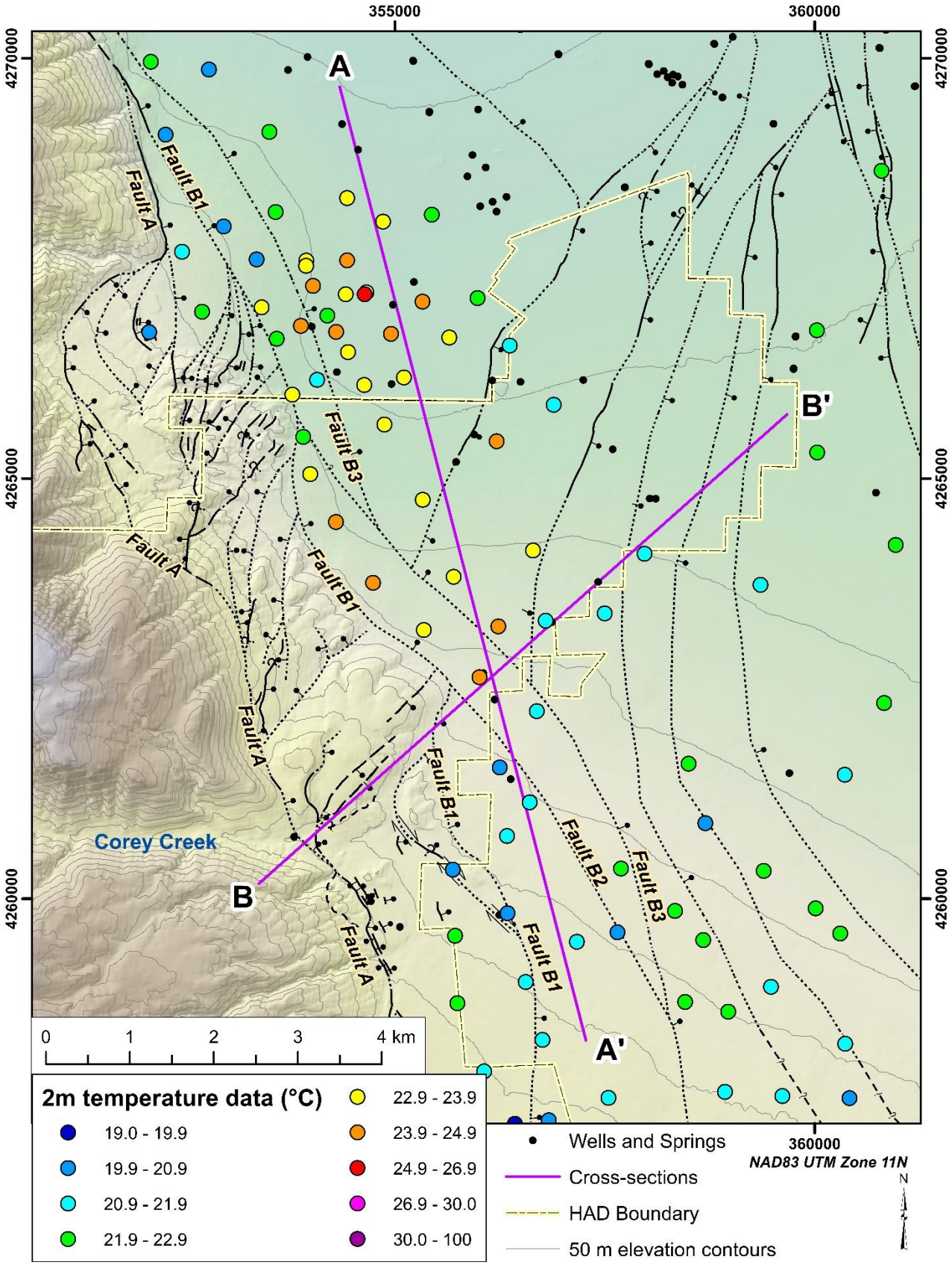

Figure 5: Map of 2 m temperature measurements previously acquired in prospect A. Temperature anomalies are observed to the north of cross section B – B' and are inferred to be associated with a shallow outflow plume of warm geothermal fluids.

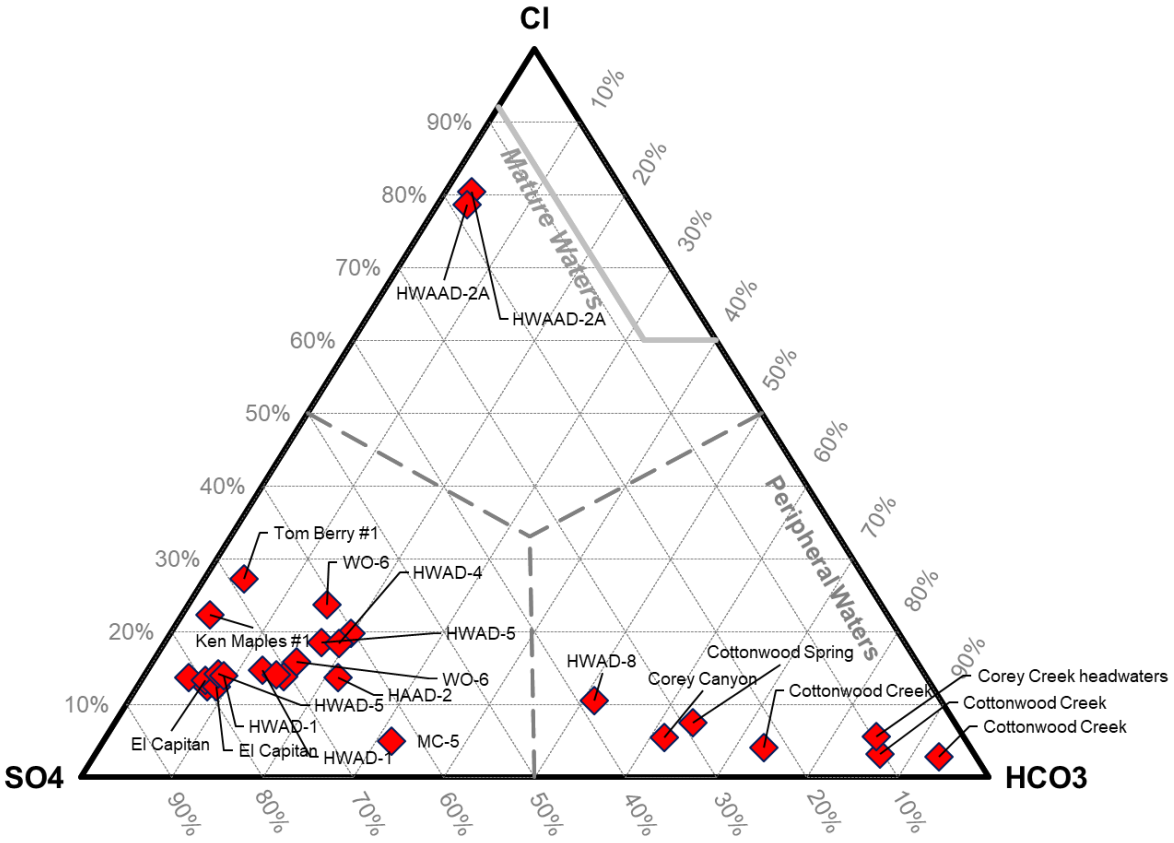

Figure 6: Trilinear plot illustrating the three fluid types at Hawthorne.

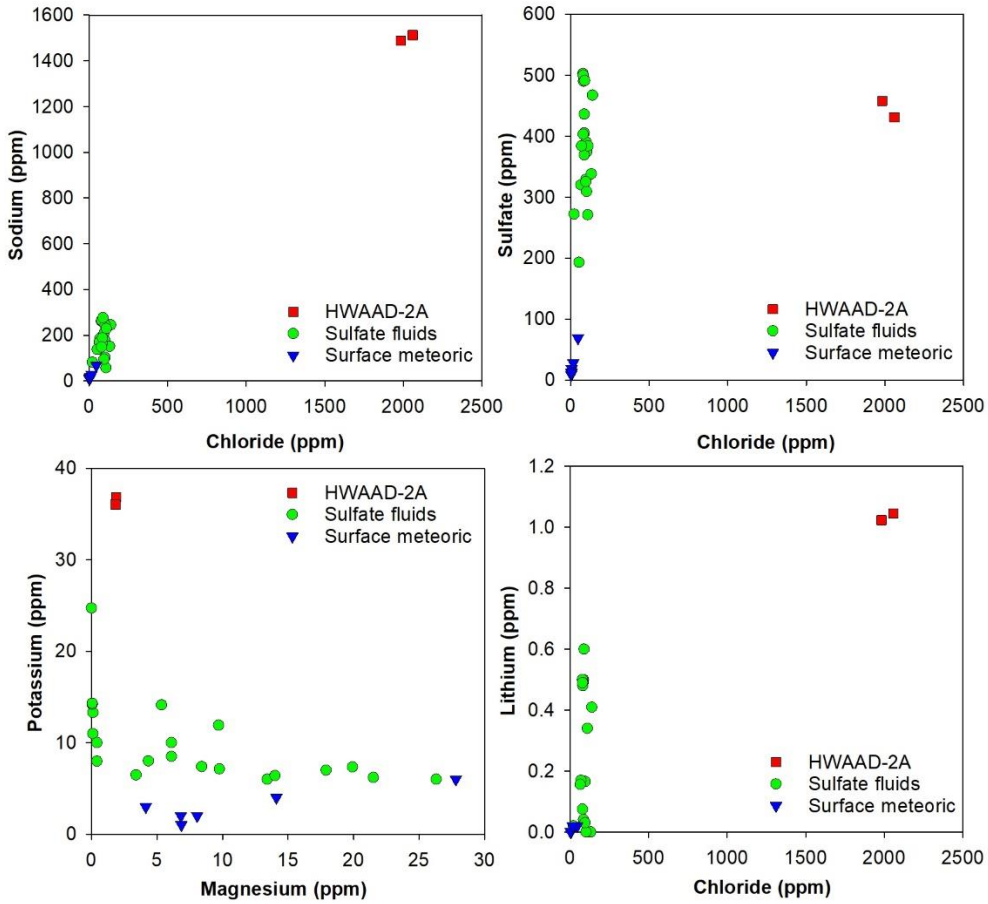

Figure 7: Geochemistry cross plots illustrating the three fluid types encountered in geothermal prospect A at Hawthorne.

For our study, only samples from the hottest wells (HWAAD-2A and El Capitan) were selected for geothermometry, as it is likely these samples have been least affected by cooling or mixing after leaving the reservoir and may provide the most reliable estimates of equilibration temperatures in the reservoir(s). The quartz geothermometer estimates equilibration temperatures of around 117 – 125 °C, which is a maximum of 10 °C warmer than the hottest measured temperature at Hawthorne (at the bottom of the HWAAD-2A well) (Table 1). Most of the fluids sampled in the basin (i.e.: the sulfate fluids and surface meteoric waters) are not mature, equilibrated alkali-chloride fluids and are thus unsuitable for conventional cation geothermometry. However, application of the conventional cation geothermometers for HWAAD-2A indicate a range of equilibration temperatures, ~120-140 °C). Multi-component equilibrium modelling was conducted to provide further constraint on possible equilibration temperatures using the GeoT code (Spycher et al., 2014) and mineralogy constraints in the reservoir from XRD analyses (Jones and Moore, 2012). The results for both the El Capitan and HWAAD-2A well are similar, and suggest temperatures no greater than 120 °C. Thus the various approaches suggest that the fluids are equilibrating somewhere between ~120 – 140 °C, and there are no obvious indications of a substantially hotter (>150 °C) system nearby.

Table 1: Geothermometry estimates for representative fluid samples at Hawthorne prospect A.

Sample Name	Max measured T (°C)	Quartz conductive	Quartz adiabatic	Na-K-Ca	Na/K Fournier 1979	Na/K Giggenbach 1988	K/Mg Giggenbach 1988	GeoT simulations
HWAAD-2A	115	118.7	116.9	137.4	119.6	139.8	122.5	117-119 ± 15
El Capitan - HAW6	98.4	122.6	120.2	97.7	152.9	171.9	136.3	120 ± 6
El Capitan - ECT11	98.4	125.3	122.5	152.1	169.2	187.4	157.5	120 ± 6

4.4 Fracture properties and stress

Acoustic image logs were acquired in the two deep wells in prospect A (HWAAD-2A and HWAAD-3) in 2009, to map the fractures in these wells and evaluate the sub-surface stress regime (Blake et al., 2011). In HWAAD-2A, both natural fractures and drilling-induced structures were identified in the image log, although only tensile fractures and petal-centerline fractures were identified (no borehole breakouts). From 1403 identified natural fractures, the mean fracture strike orientation was calculated as ~030˚, which is similar to the direction of maximum horizontal stress in other areas of the Walker Lane region of the western Great Basin where the stress direction is rotated 20 to 30° clockwise from the central Basin and Range, which is typically ~010° (Faulds et al., 2014). The average minimum principal stress orientation based on 472 identified structures was ~130°±24; this orientation rotated with depth - between 300-600 m depth, the average minimum principal stress orientation was 142°±22, whereas from 600-1300 m depth it was 121°±18 (Blake, 2011). In well HWAAD-3, 618 natural fractures were identified with an average strike of 030°, in agreement with the data from HWAAD-2A, however fewer induced fractures were identified (< 20). Overall, well HWAAD-2A had substantially more natural and induced fractures, which may reflect closer proximity to a fault intersection and/or lithologic differences due to greater intersection with the Mesozoic basement (Figure 8).

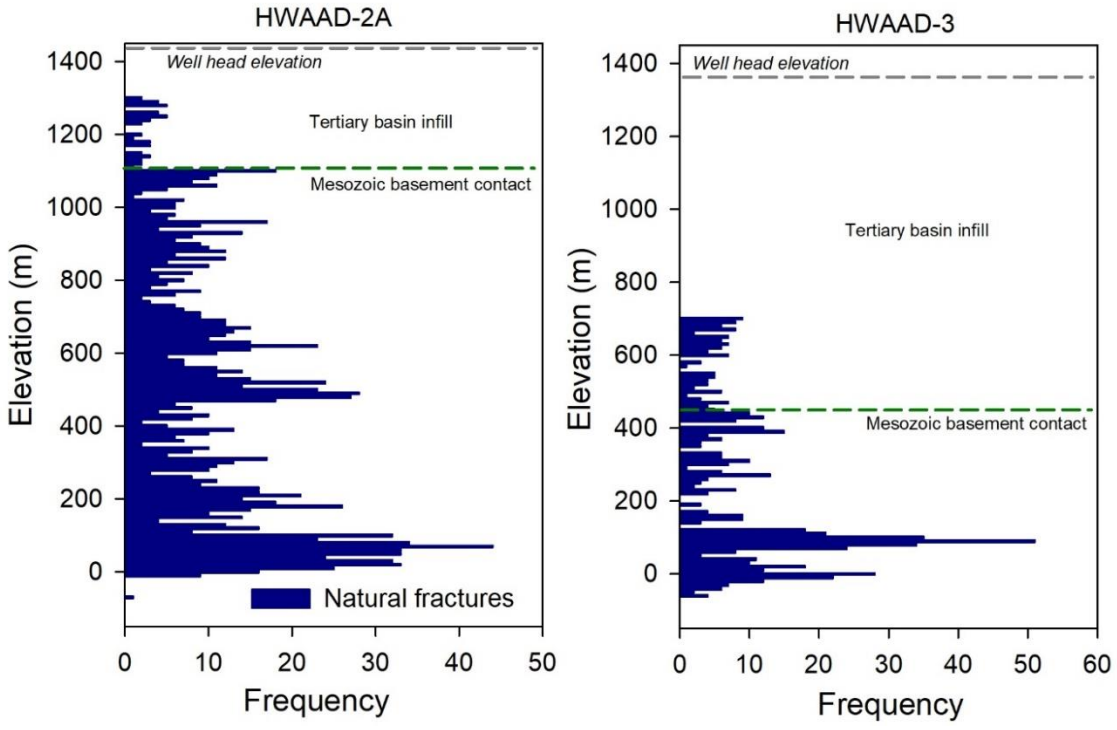

Figure 8: Frequency of natural fractures plotted against elevation in the two deep exploration wells in prospect A, identified from the acoustic logs acquired for both wells in the open-hole sections of the wells, and their relationship to lithology. Bin sizes are 10 meters.

4.5 Well test results

Well tests have been performed on some of the wells in prospect A and indicate promising productivity for possible direct-use applications (Table 2). A short pump test was performed on HWAAD-2A in 2009, and the well was found to be very productive with a productivity index (PI) of 9 gpm/psi (values above ~ 1 gpm/psi are usually considered to be commercial). Additionally, the production was solely sourced from the Mesozoic basement: the well is cased into the basement, and temperature-pressure-spinner data indicate that the main production zone is at ~ 1359 m depth in the well. During this pump test, two fluids were sampled for geochemical analyses (presented in section 4.3), thus it is assumed these samples originated from this depth. The El Capitan well was pump tested in 1981 for a longer period and higher flow rate. As mentioned previously, this well is completed in the basin infill, and produces sodium sulfate fluids. The well is cased for its full depth (305 m), however the casing is perforated from 180 m to the bottom of the well, thus it is presumed that fluids are being produced from this interval. This test indicated that the drawdown levels with a pumping rate of 532 gpm were not excessive, and the well could sustain this level of production (Koenig et al., 1981b).

Table 2: Well testing data for wells in geothermal prospect A

Well	Production fluid T (°C)	Well depth (m)	Test date	Test type	Test duration	Pump rate (gpm)	Productivity (gpm/psi)	Aquifer transmissivity	Comments
HWAAD-2A	97	1433	Mar-09	Constant rate	315 minutes	189	9	-	GeothermEx report
El Capitan	99	305	Sep-81	Constant rate	10 days	532	-	56,00 gals/day/ft width of aquifer	Koenig et al., 1981,
HWAD-1 (NAD-1)	51	105	Apr-77	Constant rate	86 hours	1500	-	40,000 sq ft/day	Bohm and Jacobson, 1977b

5. RESULTS

5.1 Describing our conceptual model

The various subsurface datasets were integrated and used to populate geological cross section across prospect A. These informed and assisted with the development of our conceptual model. The key components included in the cross sections were fault locations, lithologic contacts, well locations and depths (projected to the section when needed), temperature-depth points (used to build isotherms), and water table depth. Two cross section orientations were selected to maximize the intersection with well locations (and thus measured data points), as well as to capture the variability in thermal regime, and structural fabric: cross section A-A' (north to south), and B-B' (southwest to northeast) (Figure 9, 10). For each cross section, we created three probabilistic models with a log-normal size distribution: P90, P50 and P10. The P90 model is the most conservative (i.e.: a 90% chance that the proposed model exists in reality), the P50 model is the most 'reasonable' model that is consistent with the available data, and the P10 model is the most optimistic (i.e.: a 10% chance that the proposed model exists). The key differences between the models are the positions of the isotherms, and inferred extent of geothermal fluid upflow and outflow. Here we summarize the conceptual model for the P50 model.

A deep (>1.5 – 2 km) convective, moderate-temperature (~115-120 °C) resource composed of mature, alkali-chloride fluids is the primary heat source for a shallow (<400 m depth), cooler (90-100 °C), sulfate-fluid resource. The two reservoirs are compartmentalized, and not intermixing as indicated by their distinct chemical compositions: heat is transferred from resource 1 to resource 2 via conduction, in a 'hot plate' model. The deep resource is hosted in altered, fractured Mesozoic granite, while the shallow resource is hosted in Tertiary and Quaternary basin infilling sediments and volcanics (andesites and basaltic andesites) that date back to ~14 Ma. The sulfate fluid composition of the shallow resource is interpreted to reflect dissolution of gypsum deposits in the basin infill, or oxidation of pyrite in the Tertiary volcaniclastics that form part of the basin infill. The deep resource is associated with a bend and/or local step-over in fault B1 that may contribute to increased dilation tendency given the current stress regime. In addition, fault B1 intersects NE-striking faults in the same area, thus the structural setting is complex, and likely a hybrid structural setting. Permeability for the shallow resource is likely associated with primary permeability in the basin infilling materials, such as coarse fan-glomerates and sediments.

The deep fluid upwells on one or more fault strands associated with fault B1 in the area near HWAAD-2A. This fluid does not reach the surface or directly interact with the shallow (sulfate) fluid. Instead, it appears to conductively transfer heat to the shallow fluid across an impermeable barrier that may be associated with a fault contact and/or lithological boundary (granite vs basin infill) and/or alteration zone in the granite. The deep fluid is speculated to then flow in a NW direction at depth, bounded by the B2 and A faults. No thermal signature of the deep fluid is observed in well HWAAD3 to the east. It is possible that the deep fluid could also be flowing to the SW, but still bounded by faults B2, B1 and A. This area is associated with complex fault bends and step-overs, and the deep thermal signature could be masked by shallow water flow out of Corey Canyon. There are limited data in this area to constrain the thermal regime at depth. The deep fluid is apparently not intersected in any other well in the area given the geochemistry constraints.

The shallow fluid is meteoric water that originates in the Wassuk Range and percolates through the alluvium and fan-glomerates in the basin to form a shallow aquifer. This aquifer is locally heated by the upwelling of the deep fluid in the vicinity of HWAAD-2A/Ken Maples-1/ El Capitan. Permeable sedimentary zones in the lower part of QTsv between Fault B2 and B3 allow up-dip buoyant flow, which results in the 110 °C and 100 °C isotherms bulging diagonally upward and outward to east (Figure 10). This provides a broader heating plate for the shallow reservoir that is intersected by the Ken Maples-1 and El Capitan water wells. The heated fluid then flows in a northerly direction in a vertically constrained plume at shallow depths (<250 m), and is observed to cool off with

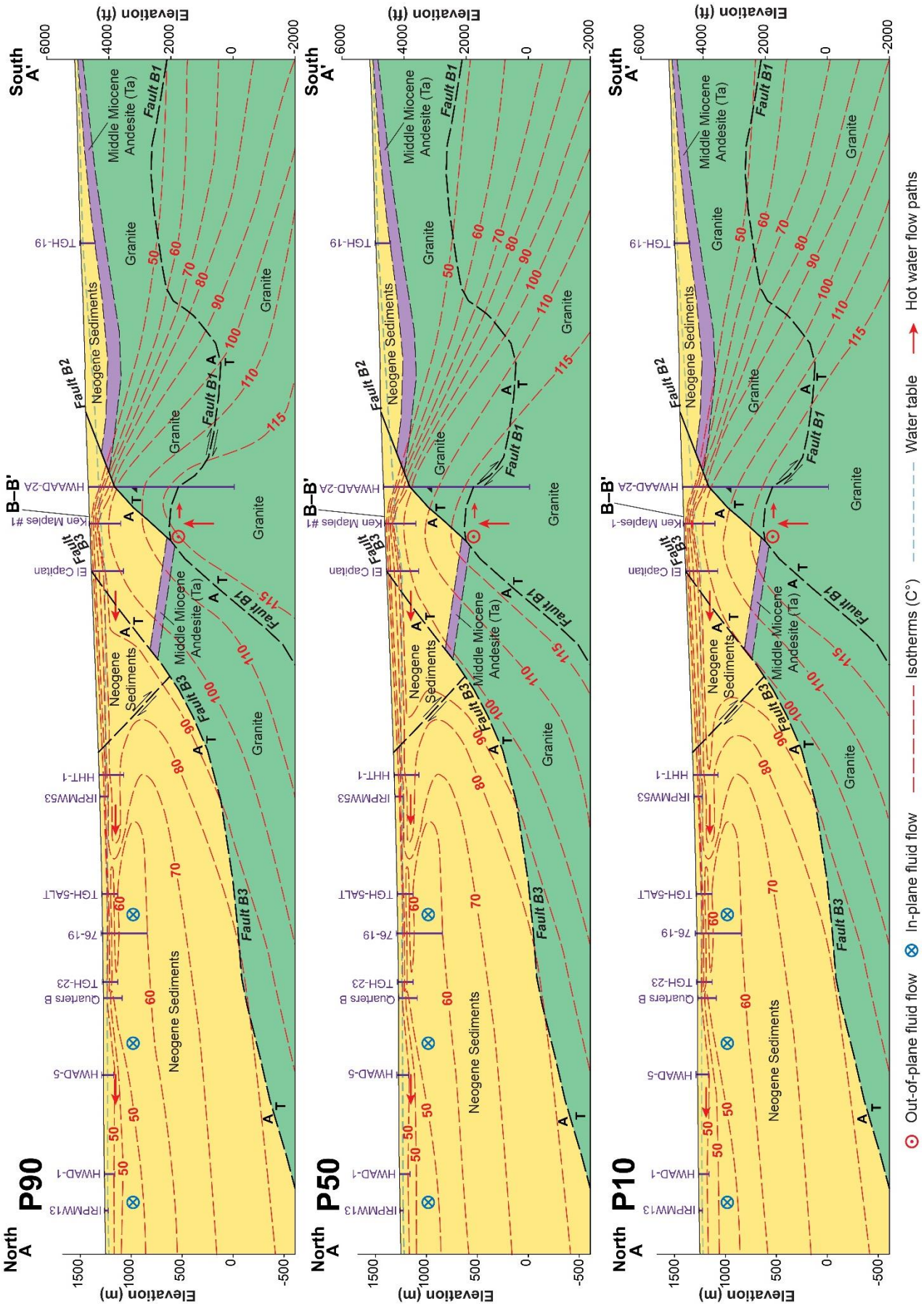

Figure 9: Cross section A – A' (north to south) across prospect A, Hawthorne Nevada. Interpreted isotherms are in dashed red lines in °C, red arrows indicated interpreted fluid flow directions, and black lines (solid and dashed) lines represent inferred fault intersections with the cross section plane.

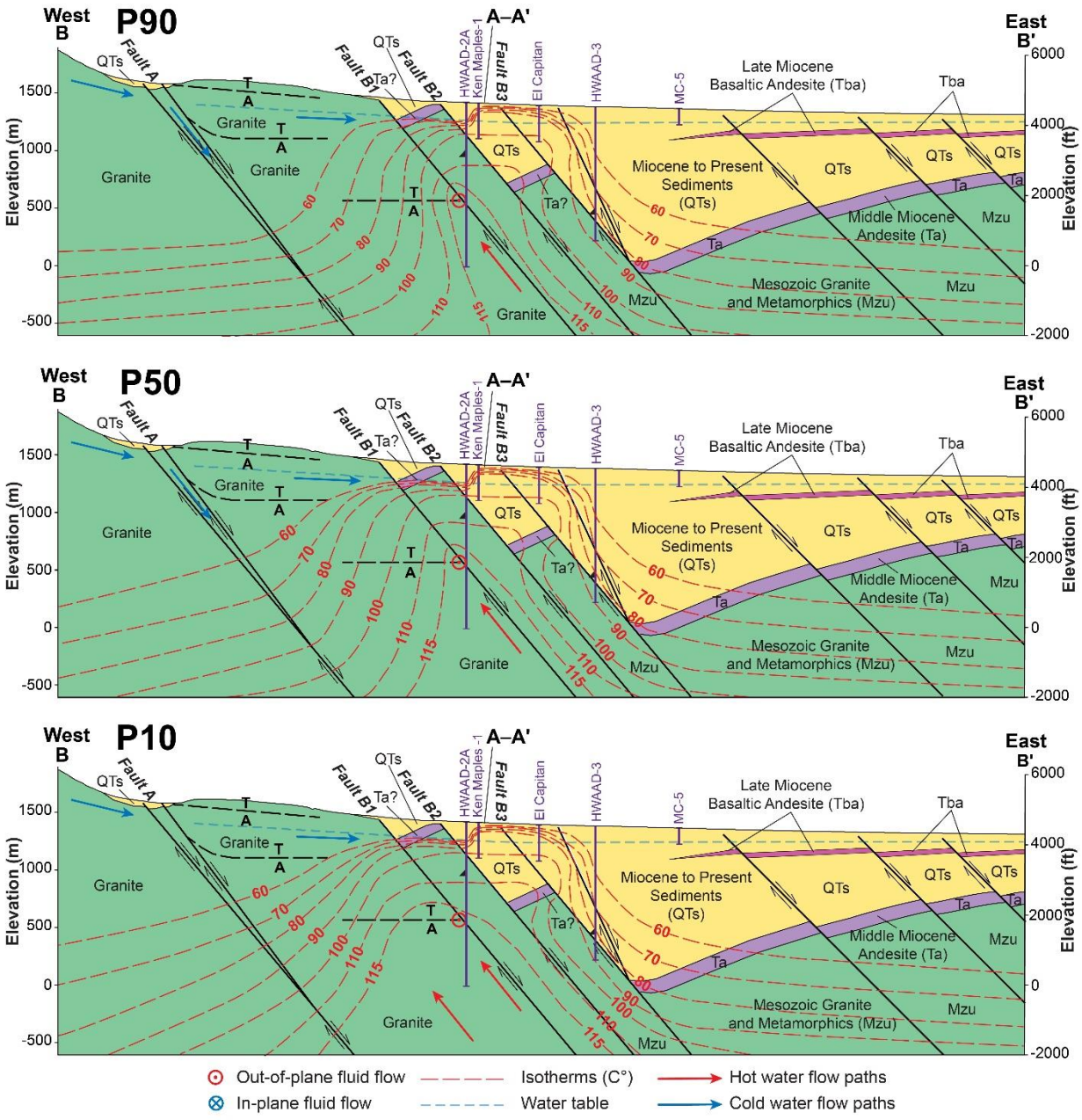

Figure 10: Cross section B – B' (south-west to north-east) across prospect A, Hawthorne Nevada. Interpreted isotherms are in dashed red lines in °C, red arrows indicated interpreted fluid flow directions, and black (solid and dashed) lines represent inferred fault intersections with the cross section plane.

distance from the El Capitan well. The plume appears to be intersected/interacting with possible shallow cold groundwater that may be flowing into the basin infill from the Wassuk Range (in the vicinity of wells TGH-5, Quarters B, 76-19, TGH-23). Also, 'lensing' of the basin sedimentary infill appears to separate the plume in places (i.e.: double over-turns are observed in the temperature logs for wells TGH-5, and Quarters-B; refer to Figure 4). The shallow warm plume does not appear to be flowing to the south or the east, as constrained by temperature gradient data in wells HWAAD-3 and MC-5. Shallow 2 m temperature data show anomalies in the vicinity of the TGH-5, TGH-23 and 76-19 wells (Figures 3 and 5). This is speculated to reflect a shallower water table compared to the south near El Capitan and in between. A shallower water table results in a thinner vadose zone and more effective heat conduction to the surface. In contrast, the area to the south has a deeper water table, thus thicker vadose zone, and less prominent 2 m anomaly. More 2 m data are required to verify this trend.

5.2 Details and assumptions for the P50, P90 and P10 conceptual models

All models (P10, P50, P90) agree with existing available data, however the P10 model is the most optimistic and the P90 model is the most conservative. Here we outline the subtleties of our models for each cross section.

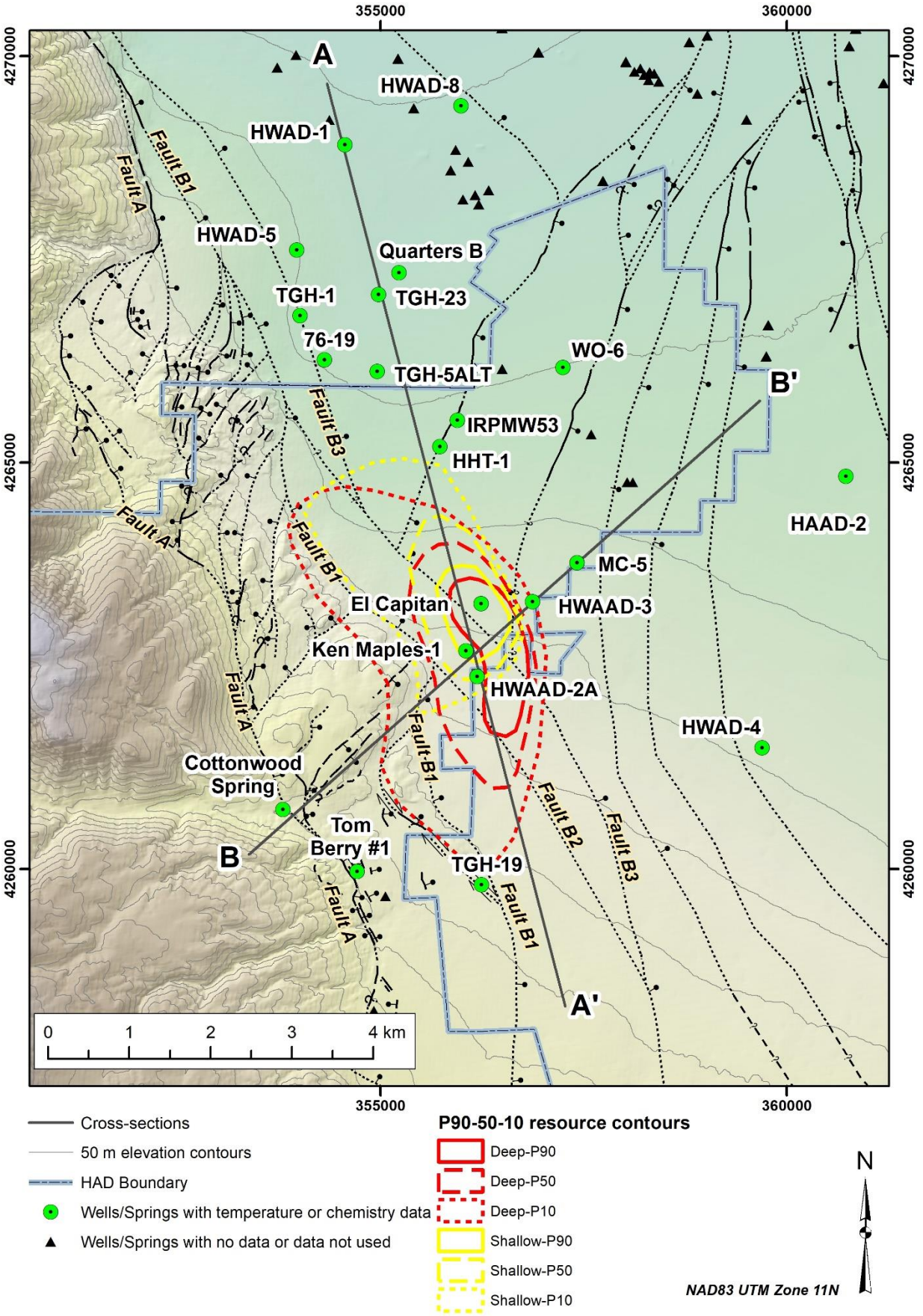

Figure 11: P90-50-10 outlines for the deep and shallow resources at Hawthorne prospect A: the deep resource outline was derived from the intersection of the 115 °C isotherm and a 2000 m depth slice, and the shallow resource outline was derived from the intersection of a 90 °C isotherm and a 250 m depth slice.

5.2.1 Deep resource details

In cross section B – B' (south-west to north-east), for the P90 scenario the upflow is restricted to fault B1 and is very narrow (Figures 10 and 11). Also, the isotherms are depressed on the west by cold water down-flow along fault A. For the P50 scenario, upflow is largely restricted to fault B1, but no cool water is flowing down Fault A. In the P10 scenario, upflow is along fault B1, in addition to synthetic cross faults west of B1, and no cool water down-flow is occurring along fault A.

In cross section A – A' (north to south) for the P90 scenario, upflow is very restricted to the B1 fault strand, and occurs right at the apex of the bend of this fault (also coincident with the intersection of fault B1 and B2) (Figure 9). In the P50 scenario, upflow is restricted to the apex of the fault bend in B1, but has a broader zone of upflow along the bend of fault B1. In the P10 scenario, upflow occurs on cross faults and synthetic faults between fault B1 and A. The range in the P10-P90 estimates ultimately reflect how much along the strike of fault B1 upflow is happening, as well as the width of the upflow zone (constrained to fault B1 or also occurring along fracture zones between fault A and B1).

5.2.2 Shallow resource details

In cross section B – B' (south-west to north-east), for the P90 scenario, the resource is proven by the El Capitan and Ken Maples-1 wells (90-100 °C fluid) in a thick section of basin infill. The location is immediately above the proposed P90 upflow of the deep resource (Figures 9, 10 and 11). In the P50 scenario, the resource/reservoir extends all the way to fault B1 (west of Ken Maples-1 and El Capitan): this is the stratigraphic limit of any appreciable thickness of basin fill (<10 m) that is thought to be the primary reservoir for the shallow resource. Also, any sediments west of B1 are above the water table. For the P10 scenario, the resource/reservoir extends halfway to fault A, and is consistent with the P10 for the deep resource in which upflow is distributed along several cross faults/synthetic faults/fractures in between B1 and A that could conductively heat a shallow resource. The shallow resource would need to be hosted in a fracture zone at the top of the granite given the lack of sediment basin infill in this area. This would in turn also require a clay-cap barrier in the granite to hydraulically isolate the deep chloride fluid from the shallow fluid.

In cross section A – A' (north to south), the P90-10 estimates reflect difference in the area of potential conductive heat-transfer from the deep resource. The temperatures are constrained at the surface in the south by the top of HWAAD-2, and in the north by HHT-1. For the P90 scenario, the resource/reservoir is restricted to a narrow zone around Ken Maples-1 and El Capitan. In the P50 scenario, the resource/reservoir extends halfway between the El Capitan and HHT-1 wells. In the P10 scenario, the resource is more laterally extensive, reflecting a greater heat-conduction area from the deep resource. The isotherms are constrained at the northern end by measured temperatures in HHT-1.

6. DISCUSSION

6.1 Conceptual model uncertainties and questions

There are several remaining questions about the subsurface characteristics of prospect A that affect the certainty of some aspects of our proposed conceptual model.

6.1.1. Faults

Subsurface fault properties in prospect A are somewhat constrained by a 3D seismic model to the south, surface measurements, and fault intersections in the deep wells HWAAD-2A and HWAAD-3. The fault dips are constrained by the 3D seismic model, and >50 measurements along the surface trace of fault A. Surface traces of faults B1, B2 and B3 are inferred through the extrapolation of interpreted fault intersections in wells HWAAD-2A and HWAAD-3, and the 3D seismic survey to the south. From down-hole observations, the intersection of fault B2 and HWAAD-2A is well constrained, and intersection of fault B3 with HWAAD-3 is well constrained. There are multiple circulation losses in HWAAD-2A that could correspond to fault B1.

Remaining questions include constraining the precise location and dips of faults B1, B2 and B3: these are all concealed faults under alluvium. The seismic data are relatively noisy and could be reprocessed with more advanced algorithms to improve the quality of the fault picks. The extension of the Hawthorne fault zone to the south is also uncertain (i.e.: do faults B1 and B2 terminate against fault B3, or continue out to fault A? – refer to Figure 3 for fault locations). The southern ends of these faults are also concealed. As constrained by gravity data, the Hawthorne fault zone does not have a large cumulative offset (est. < 100 m). The segments that are not concealed were active in the Holocene, as they cut Lake Lahontan shorelines. Future work involving coupled gravity – magnetic inversions may help to improve the mapping of the concealed, sub-surface faults in the basin.

6.1.2 Fluid source, chemistry and flow pathways

Even with the extensive sub-surface well dataset that is available at Hawthorne, key questions remain pertaining to the origin and subsequent flow path of the deep geothermal fluid (alkali-chloride), which is only detected in well HWAAD-2A (>1300 m depth). We presume that this fluid represents deep, long-circulation meteoric water from the Wassuk Range that has percolated through permeable faults to depths > 2 km, is heated, and returns to the surface via other permeable faults (proposed as fault B2). We know that the fluid is likely flowing up a fault in the vicinity of HWAAD-2A, but which segment dominates, and is the deep fluid flowing up the fault for a distance along-strike (e.g.: to the north)? The other question is where does this fluid go? Samples collected from shallow (<400 m deep) wells in the basin show no evidence of mixing with this alkali chloride fluid. We speculate that this deep fluid could flow through the fractured Mesozoic basement (or along faults) either to the north or south of our interpreted upflow location near HWAAD-2A, but this is unconstrained.

6.1.3 Temperature data

There are some data gaps in the temperature dataset – both spatially, and with depth. There are limited temperature logs that are deeper than 300 m (only three). The hottest wells for the shallow geothermal resource (El Capitan and Ken Maples-1) do not have full temperature logs – only a partial log (El Capitan), or a single measurement at a given depth (Ken Maples-1). In terms of spatial data coverage, there are limited wells to the south and west of our interpreted upflow location near HWAAD-2A, and a gap in between El Capitan to HHT-1 (refer to Figure 3). New temperature log data from deep wells to the south, west and along strike (north) with

fault B2 would help to constrain the size of the deep geothermal upflow, and also its potential outflow direction. Infill data in between El Capitan and HHT-1 would provide further confidence/confirmation as to the extent and nature of the shallow outflow plume.

6.2 Comparison with earlier proposed conceptual models at Hawthorne

Our updated conceptual model of the geothermal system associated with Hawthorne prospect A builds on almost 40 years of exploration and analysis by previous researchers, and includes some of the same aspects and relationships that were first proposed in the late 1970's. However, due to additional data collection and new data integration approaches, we have been able to develop a new model that is more quantitative and honors the thermodynamic constraints (still with uncertainties as discussed above in section 6.1). Also, we have identified new, previously unrecognized components to the geothermal system at prospect A. Key similarities include the assertion that fault intersections have a controlling location on geothermal upflow, and that there is a sodium-sulfate rich fluid that is flowing through the basin infill from south to north. Key differences in our model arise due to the new data acquired in HWAAD-2A and HWAAD-3. These wells were instrumental in constraining the deep thermal regime as well as documenting the existence of a chemically distinct, deep geothermal fluid that is hosted in the Mesozoic basement. On the basis of the temperature log data, and chemistry data from shallow wells that are producing sodium-sulfate fluids, we infer that the deep geothermal system (characterized by an alkali chloride fluid) is conductively heating the shallow aquifer above. This is a radically different model to previous studies, and its inception is almost entirely due to the drilling, logging, sampling and flow testing the two deep wells HWAAD-2A and HWAAD-3.

7. SUMMARY

The Hawthorne area has been investigated for its geothermal potential for over 40 years: during this time, multiple datasets have been acquired. We re-evaluated and synthesized available sub-surface data to develop a new conceptual model of prospect A, which is located at the base of the Wassuk Range, west of the town of Hawthorne. Key findings include identifying two compartmentalized geothermal fluids that are not in direct contact. Instead it appears that a deeper, mature alkali-chloride fluid hosted in Mesozoic granite is conductively transferring its heat to a shallower, sodium-sulfate fluid that is hosted in Tertiary basin infill. Resource temperatures at depth are inferred to be no greater than ~120 °C (up to a possible maximum of 140 °C) on the basis of chemical geothermometry. The shallow resource (sulfate fluid) forms a thermal outflow plume that flows in a northerly direction from the presumed heat-transfer zone with the deep resource (in the vicinity of the El Capitan well). This shallow fluid cools with increasing distance from the upflow. The outflow location of the deep alkali-chloride fluid is unconstrained, and it may continue to flow at depth through the Mesozoic basement either to the north or south of the inferred upflow location. Further infill drilling to the north, west and south of the HWAAD-2A and El Capitan well would reduce the uncertainty about the size and extent of the deep geothermal upflow along concealed faults in the basin (fault B1), as well as constrain its outflow direction.

ACKNOWLEDGEMENTS

This work was performed under a subcontract with Sandia National Laboratories and funded by the United States Department of Energy Geothermal Technologies Office. The conceptual model development benefited from initial discussions and advice from Bill Cumming.

REFERENCES

Arguello, R., Schwendig, J., Lowry, T., Sabin, A., Blake, K., Lazaro, M., Anderson, S., Ayling, B., Tiedeman, A., Hinz, N.: Deep direct-use geothermal: development of a demand-side model for the Hawthorne, Nevada area. *Transactions*, Geothermal Resources Council, **42**, (2018), 7p.

Bell, J.W., and Hinz, N.: Young Walker Basin faults provide new insights into structural relations controlling geothermal potential at the Hawthorne Army Weapons Depot, central Nevada. *Transactions*, Geothermal Resources Council, **34**, (2010), 751-754.

Blake, K.: HWAAD-2A and HWAAD-3: Fracture and Stress Analysis, Hawthorne Army Deport, Hawthorne, NV Initial Assessment. Internal Navy Geothermal Program Office Technical Report, (2011), 18p.

Blake, K., Sabin, A., Lowry, T.S., Lazaro, M., Tiedeman, A., Ayling, B., Arguello, R., and Meade, D.: Hawthorne Army Depot: Update of geothermal exploration and direct use applications. *Transactions*, Geothermal Resources Council, **41**, (2017), 11p.

Bohm, B.W., and Jacobson, R.L.: Preliminary investigation of the geothermal resources near Hawthorne, Nevada. Water Resources Center, Desert Research Institute, Project Report No. 50, (1977a), 35p.

Bohm, B., and Jacobson, R.L.: Results on the pump test of NAD 1, Water Resources Center, Desert Research Institute, (1977b).

Faulds, J.E., and Henry, C.D.: Tectonic influences on the spatial and temporal evolution of the Walker Lane: An incipient transform fault along the evolving Pacific – North American plate boundary, in Spencer, J.E., and Titley, S.R., eds., Ores and orogenesis: Circum-Pacific tectonics, geologic evolution, and ore deposits: *Arizona Geological Society Digest* **22**, (2008), 437-470.

Faulds, J.E., Hinz, N.H., and others: Characterizing Structural Controls of EGS-Candidate and Conventional Geothermal Reservoirs in the Great Basin: Developing Successful Exploration Strategies in Extended Terranes: Final report submitted to the Department of Energy, (2014), 54 p.

Fournier, R.O., A revised equation for the Na/K geothermometer. *Transactions*, Geothermal Resources Council, **3**, (1979), 221-224.

Geothermal Development Associates (GDA): A preliminary plan for the development of geothermal energy in the town of Hawthorne, Nevada. Prepared by GDA for Nevada Department of Energy, (1981), 109 p.

GeothermEx: Memorandum: Rig test of Hawthorne well HWAAD-2A. Prepared for the Navy Geothermal Program Office by GeothermEx, 31 March 2009, (2009), 6 p.

Giggenbach, W.F., Geothermal solute equilibria: Derivation of Na-K-Mg-Ca geoindicators. *Geochimica et Cosmochimica Acta* **52**, (1988), 2749–2765.

Hardyman, R.F., and Oldow, J.S.: Tertiary tectonic framework and Cenozoic history of the central Walker Lane, Nevada, in Raines, G.L., ed., Geology and Ore Deposits of the Great Basin: Reno, Geological Society of Nevada, (1991), 279-302.

Hinz, N.H., Faulds, J.E., Moeck, I., Bell, J.W., Oldow, J.S.: Structural controls of three blind geothermal resources at the Hawthorne Ammunition Depot, west-central Nevada. *Transactions*, Geothermal Resources Council, **34**, (2010), 785-790.

Jones, C., and Moore, J.: Petrographic and X-ray Diffraction Study of 3 Wells from the Hawthorne Ammunition Depot, Mineral County, Nevada. Report prepared by the Energy and Geoscience Institute for the Navy Geothermal Program Office, (2012).

Katzenstein, A., Bjornstad, S., Meade, D., 2002. Geothermal resource evaluation of the Hawthorne Army Ammunition Depot (HWAD), Hawthorne, NV. Internal report, Navy Geothermal Program Office, Chine Lake, CA. 31pp.

Kell-Hills, A., Louie, J., Kent, G., Pullammanappallil, S., Sabin, A., Lazarro, M.: A revised interpretation of 3D seismic data, Hawthorne Army Depot, Nevada: faulted-basin reflections or sill intrusions? *Transactions*, Geothermal Resources Council, **34**, (2010), 869-872.

Koenig, B.A.: Hawthorne Study Area. *In:* Low-to-moderate temperature resource assessment for Nevada: Area specific studies., by Trexler, D.T., Koenig, B.A., Flynn, T., Bruce, J.L., Ghusn, G., Final report to the US Department of Energy, prepared by the University of Nevada, Reno under contract No. AC08-79NV10039, (1981), 224p.

Koenig, B.A., Flynn, T., and Bruce, L.P.: Pump test of El Capitan Geothermal Well, Hawthorne, Nevada. Prepared for Nevada Department of Energy, (1981), 34p.

Kratt, C., Sladek, C., Coolbaugh, M.: Boom and bust with the latest 2m temperature surveys: Dead Horse Wells, Hawthorne Army Depot, Terraced Hills, and other areas in Nevada. *Transactions*, Geothermal Resources Council, **34**, (2010), 567-573.

Lazaro, M., Page, C., Tiedeman, A., Sabin, A., Bjornstad, S., Alm, S., Meade, D., Shoffner, J., Mitchell, K., Crowder, B., GBCGE, and Halsey, G.: United States Department of the Navy geothermal exploration leading to shallow and intermediate/deep drilling at Hawthorne Ammunition Depot, Hawthorne, NV. *Transactions*, Geothermal Resources Council, **34**, (2010), 595-598.

Meade, D., Lazaro, M., Bjornstad, S., Alm, S., Tiedeman, A., Sabin, A., Page, C.: Results of the US Navy Geothermal Program Office 2010 drilling project at Hawthorne Army Depot, Nevada. *Transactions*, Geothermal Resources Council, **35**, (2011), 193-195.

Moeck, I., Hinz, N., Faulds, J., Bell, J., Kell-Hills, A., Louie, J.: 3D geological mapping as a new method in geothermal exploration: A case study from central Nevada. *Transactions*, Geothermal Resources Council, **34**, (2010), 807-811.

Oldow, J.S.: Late Cenozoic displacement partitioning in the northwestern Great Basin, *in* Craig, S.D., ed., Structure, tectonics, and mineralization of the Walker Lane: Reno, Nevada, *Proceedings*, Geological Society of Nevada Symposium, (1992) 17-52.

Penfield, R., Zehner, R., Coolbaugh, M., Shevenell, L., Hastings, J., Johnson, G., Snyder, W., Morgos, D., Kurz, K., Sabin, A., Lazaro, M., Bjornstad, S., Halsey, G.: Geothermal site assessment using the National Geothermal Data System (NGDS), with examples from the Hawthorne ammunition depot area. *Transactions*, Geothermal Resources Council, **34**, (2010), 709-714.

Proffett, J.M., Jr.: Cenozoic geology of the Yerington district, Nevada, and implications for the nature and origin of basin and range faulting: *Geological Society of America Bulletin*, **88**, (1977), 247-266.

Proffett, J.M., and Dilles, J.H.: Geologic map of the Yerington district: Nevada Bureau of Mines and Geology Map 77, scale 1:24,000, (1984).

Robinson, S., and Pugsley, M.: Geothermal resource area 8 – Mineral and Esmeralda Counties, Area Development Plan. Nevada Department of Energy, prepared under contract number DE-FC03080RA50075, (1981), 87p.

Sabin, A., Blake, K., Tiedeman, A., Hinz, N., Ayling, B., Lowry, T., Arguelloa, R., Lazaro, M.: Deep direct-use geothermal: production side analysis from Hawthorne, NV. *Transactions*, Geothermal Resources Council, **42**, (2018).

Spycher, N., Peiffer, L., Sonnenthal, E.L., Saldi, G., Reed, M.H., Kennedy, B.M.: Integrated multicomponent solute geothermometry. *Geothermics*, **51,** (2014), 113-123.

Shoffner, J.D., Li, Y., Hinz, N., Sabin, A., Lazaro, M., Alm, S.: Understanding fault characteristics and sediment depth for geothermal exploration using 3D gravity inversion in Walker Valley, Nevada. *Transactions*, Geothermal Resources Council, **34**, (2010), 633-636.

Stewart, J.H.: Tectonics of the Walker Lane belt, western Great Basin: Mesozoic and Cenozoic deformation in a zone of shear, *in* Ernst, W.G., ed., The Geotectonic development of California: Prentice Hall, Englewood Cliffs, New Jersey, (1988), 683-713.

Stockli, D.F., Surpless, B.E., Dumitru, T.A., and Farley, K.A.: Thermochronological constraints on the timing and magnitude of Miocene and Pliocene extension in the central Wassuk Range, western Nevada: *Tectonics*, **21(4),** (2002), 10.1029/2001TC001295.

Surpless, B.E., Stockli, D.F., Dumitru, T.A., and Miller, E.L.: Two-phase westward encroachment of Basin and Range extension into the northern Sierra Nevada: *Tectonics*, **21**(1002), (2002), doi:10.1029/2000TC001257.

Wesnousky, S.G.: Active faulting in the Walker Lane: *Tectonics*, **24**, TC3009, (2005), doi:10.029/2004TC001645.